JOC The Journal of Organic Chemistry

Article

pubs.acs.org/joc

Computational Investigation of the Aminolysis of RAFT Macromolecules

Gilles B. Desmet,[†] Dagmar R D'hooge,[†,‡] Maarten K. Sabbe,[†] Marie-Françoise Reyniers,*[,†] and Guy B. Marin[†]

[†]Laboratory for Chemical Technology and [‡]Department of Textiles, Ghent University, Technologiepark 914, 9052 Gent, Belgium

Supporting Information

ABSTRACT: This work presents a detailed computational study and kinetic analysis of the aminolysis of dithioates, dithiobenzoates, trithiocarbonates, xanthates, and thiocarbamates, which are frequently used as chain-transfer agents for reversible addition−fragmentation chain-transfer (RAFT) polymerization. Rate coefficients were obtained from ab initio calculations, taking into account a diffusional contribution according to the encounter pair model. A kinetic model was constructed and reveals a reaction mechanism of four elementary steps: (i) formation of a zwitterionic intermediate, (ii) formation of a complex intermediate in which an assisting amine molecule takes over the proton from the zwitterionic intermediate, (iii) breakdown of the complex into a neutral tetrahedral intermediate with release of the assisting amine molecule, and (iv) amine-assisted breakdown of the neutral intermediate to the products. Furthermore, a comparative analysis indicates that the alkanedithioates and dithiobenzoates react the fastest, followed, respectively, by xanthates and trithiocarbonates, which react almost equally fast, and dithiocarbamates, which are not reactive at typical experimentally used conditions.

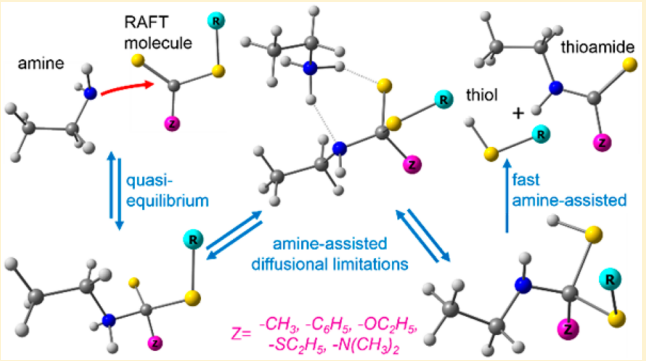

1. INTRODUCTION

The reversible addition−fragmentation chain-transfer (RAFT) polymerization process has revolutionized the field of radical polymerization.[1] It enables precise control over the molecular weight and architecture, leading to the synthesis of complex macromolecular structures, such as block copolymers, star-shaped polymers, brush polymers, comb polymers, dendrimers and cross-linked polymer networks. This control is achieved by suppressing bimolecular termination via reversible trapping of the propagating radicals with a thiocarbonylthio type of compound, as shown in Figure 1.

The effectiveness and versatility of this process depends crucially on the reactivity of the polymeric radical with these so-called RAFT agents. While these compounds lay at the core of the RAFT process, they constitute, at the same time, one of the main complications because the resulting thiocarbonylthio end groups of the polymers are prone to decomposition into malodorous sulfur-containing compounds.[2] Hence, an important property of RAFT macromolecules is the ease with which their functional end group can be transformed. This is typically done by aminolysis with either primary or secondary amines to a thiol[2−6] as shown in Figure 2.

Once a thiol has been formed, a realm of thiol−ene reactions opens (cf. Figure 2) via either a radical mechanism[7,8] or a Michael addition.[9,10] These strategies can thus not only be used to transform the RAFT end group, but can also be applied advantageously to obtain a wealth of functionalized polymers.[11−13]

Notwithstanding the plentitude of experimental studies and the many possible applications of the aminolysis of RAFT end groups, a kinetic analysis in terms of elementary steps has, to the best of our knowledge, never been presented before. Therefore, this work presents an ab initio based kinetic analysis of the aminolysis of four classes of commonly used RAFT agents, i.e., dithiobenzoates, trithiocarbonates, xanthates, and dithiocarbamates. To identify the governing reaction mechanism of the aminolysis, first the rate coefficients are calculated for all elementary reactions in a detailed reaction network that considers several competing reaction mechanisms for the aminolysis of a model RAFT agent with ethylamine. As model RAFT agent, methylethane dithioate (MEDT; see Figure 3) is used. MEDT is typically not experimentally used, but due to its small size it enables the use of highly accurate computational methods, and therefore, it has been used before as a model compound in computational studies on RAFT agents.[14−16] In a next step, rate analysis of the aminolysis of MEDT over a broad range of reaction conditions was performed to determine the governing reaction mechanism.

Once the operative mechanism is determined for this model compound, the thermodynamic and kinetic parameters for

Received: July 29, 2016
Published: November 3, 2016

DOI: 10.1021/acs.joc.6b01844
J. Org. Chem. 2016, 81, 11626−11634

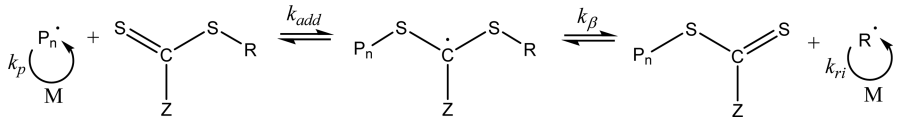

Figure 1. RAFT process: the propagating macroradical, P_n, is deactivated upon addition to a RAFT agent, forming a RAFT intermediate radical. This RAFT intermediate radical can then fragment, either releasing the original macroradical or the R group, which can then reinitiate the propagation of a new macroradical. Key: P_n, macroradical of length n; k_p, rate coefficient of propagation; M, monomer; k_{add}, rate coefficient of radical addition; k_β, rate coefficient for β-scission; k_{ri}, rate coefficient of reinitiation. Typical examples for Z groups include alkyl, aryl, alkoxy, thio, or amino groups.

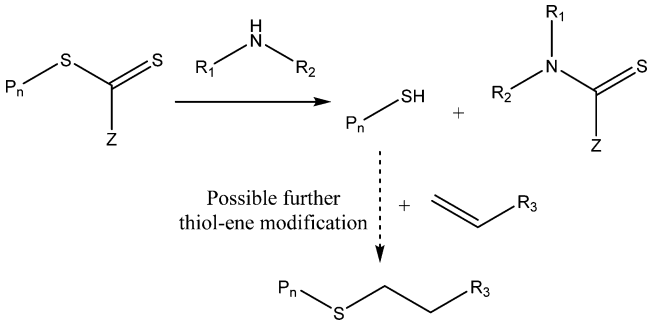

Figure 2. Aminolysis of a RAFT macromolecule leading to a thiol-functionalized polymer. P_n represents the polymer chain, Z the characterizing group for the RAFT agent. In the case where a primary amine is used, R_1 or R_2 is a hydrogen atom. The obtained thiol can be further functionalized via a thiol−ene reaction.

experimentally more representative RAFT agents are calculated, i.e., ethyl dithiobenzoate (EDTB), diethyl trithiocarbonate (DETTC), diethyl xanthate (DEX) and ethyl dimethyl dithiocarbamate (EDMDTC), as shown in Figure 3.

The calculated parameters are then used in a microkinetic model, and simulated conversions are compared with the experimental data reported in the literature. Furthermore, the reactivities of the different classes of RAFT agents are compared under similar conditions.

2. RESULTS AND DISCUSSION

Identification of the Aminolysis Mechanism Using MEDT as a Model Compound. Based on the aminolysis mechanism of analogous molecules,[17] a detailed reaction scheme for the aminolysis of a RAFT macromolecule (**T**) with ethylamine (**EA**) in an apolar solvent (THF) is presented in Figure 4.

The reaction scheme considers several competing mechanisms, and a comprehensive search of possible intermediates and transition-state structures for the different reaction mechanisms was performed at the B3LYP/6-31G(d) level of theory using MEDT as a model compound (R and Z = CH_3). Note that in the macromolecular analogous reaction R would be the polymer chain. For transition states involving proton transfer, the participation of amines and generated thiols is of major importance. It is known that the rate of aminolysis is second order in the concentration of amine, indicating that next to being a reactant, the amine also functions as a catalyst.[18,19] Additionally, generated products that contain a group which can both be proton donating and proton accepting, such as, for instance, the formed thiol (**P2**), are able to assist in proton-transfer reactions, effectively resulting in an autocatalytic type of reaction.[17,20] Note that, while the reacting primary amine and the generated thiol (**P2**) are able to assist in proton-transfer reactions due to their free electron pair and bonding with hydrogen, the generated thioamide (**P1**) does not have this capacity, since the electrons on its nitrogen are delocalized. Reaction and activation enthalpies, entropies, and Gibbs free energies for all elementary reactions for the aminolysis of MEDT at 298.15 K were calculated in THF using M06-2X/6-311G(d,p) with solvent contributions accounted for using COSMO-RS and are given in Table 1; the corresponding values in the gas phase are presented in Table S3 in the Supporting Information. Note that the Gibbs free energy barrier for **R6** is slightly negative. For reactions with these kind of flat potential energy surfaces, variational transition-state theory[21] should actually be applied to obtain accurate values for the intrinsic parameters. However, since for these reactions the apparent reaction parameters will be dominated by diffusional limitations (see further), the intrinsic parameters are of little influence, and for the further calculation of the rate coefficients (Table 2) $\Delta^{\ddagger}G^{\circ}$ of **R6** is set at 0.

The Gibbs free energy diagram shown in Figure 5 further illustrates the relation between the reactants, intermediates, and transitions states involved in the various competing mechanisms considered for the aminolysis of MEDT with **EA**.

The first elementary reaction (**R1**) is the formation of a zwitterionic intermediate (**ZI**) via nucleophilic attack of the amine (**EA**) on the thioate (MEDT). These zwitterionic intermediates have been reported to be involved in the aminolysis reactions of esters as well.[22,23] Although this reaction is exothermic, the large loss in entropy makes it endergonic overall. Once the zwitterionic intermediate is formed, it can react to the products (**P1** and **P2**) via a direct intramolecular proton transfer (**R2**) or via an amine-assisted

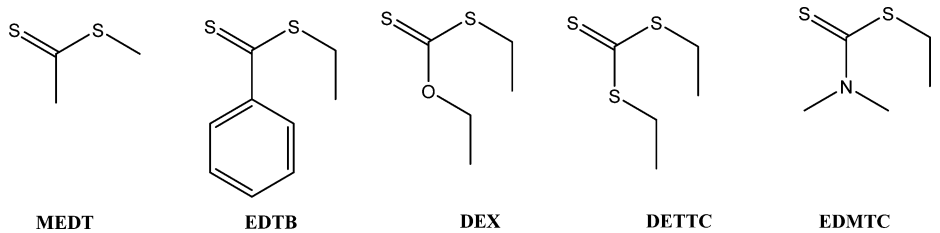

Figure 3. Chemical structures of the RAFT agents used in this study: methylethane dithioate (MEDT), ethyl dithiobenzoate (EDTB), diethyl trithiocarbonate (DETTC), diethyl xanthate (DEX), and ethyl dimethyl dithiocarbamate (EDMDTC).

DOI: 10.1021/acs.joc.6b01844
J. Org. Chem. 2016, 81, 11626−11634

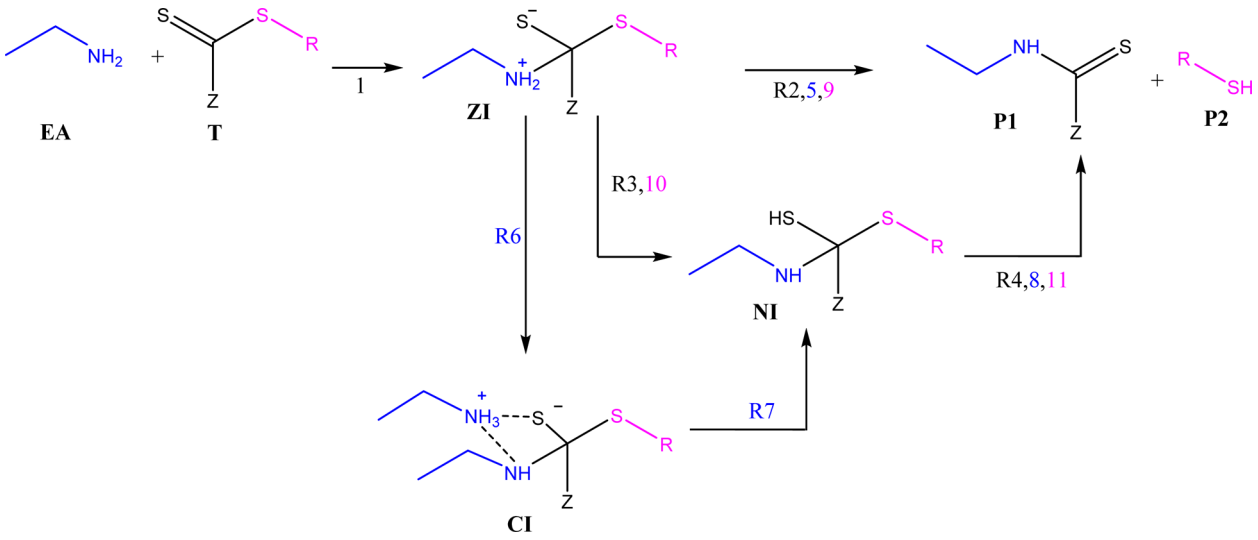

Figure 4. Reaction network for the aminolysis of a RAFT macromolecule T (in case of MEDT, R and Z = CH_3) with EA. Reactions 5−8 are assisted by ethylamine (EA) and are shown in blue, while reactions 9−11 are assisted by the thiol (**P2**) and are shown in pink.

Table 1. Standard Reaction Enthalpy, Entropy, and Gibbs Free Energy ($\Delta_rH°$, $\Delta_rS°$, $\Delta_rG°$ in, Respectively, kJ mol^{-1}, J mol^{-1} K^{-1}, kJ mol^{-1}). Standard Activation Enthalpy, Entropy and Gibbs Free Energy ($\Delta^{‡}H°$, $\Delta^{‡}S°$, $\Delta^{‡}G°$ in, Respectively, kJ mol^{-1}, J mol^{-1} K^{-1}, kJ mol^{-1}) at 298.15 K in THF[a]

reaction	$\Delta_rH°$	$\Delta_rS°$	$\Delta_rG°$	$\Delta^{‡}H°$	$\Delta^{‡}S°$	$\Delta^{‡}G°$
R1	−25.0	−198.4	34.2	−6.4	−187.4	49.5
R2	−42.5	173.2	−94.1	101.6	26.3	93.8
R3	−9.1	69.0	−29.6	86.0	50.8	70.9
R4	−33.4	104.1	−64.4	98.0	−19.0	103.6
R5	−42.5	173.2	−94.1	40.2	−65.3	59.7
R6	−23.6	−72.9	−1.9	−31.1	−97.1	−2.1
R7	14.5	141.9	−27.8	−0.4	−2.2	0.2
R8	−33.4	104.1	−64.4	−2.2	−146.1	41.4
R9	−42.5	173.2	−94.1	86.7	−68.0	107.0
R10	−9.1	69.0	−29.6	8.4	−85.0	33.7
R11	−33.4	104.1	−64.4	74.9	−39.6	86.7

[a]Reference state is 1 mol L^{-1} for all elementary reactions in the reaction network of the aminolysis of MEDT with EA, as presented in Figure 4.

(**R5**) or thiol-assisted (**R9**) proton transfer. As illustrated in Figure 6, in the transition states for these two latter cases, the assisting molecule accepts a proton from the attacking amine nucleophile and donates one of its own protons to the sulfur.

Alternatively, the zwitterionic intermediate (**ZI**) can react further to a neutral intermediate (**NI**) via an intramolecular proton transfer (**R3**) or via a thiol-assisted transition state (**R10**). In the case of amine assistance, a local minimum is detected corresponding to a stable complex intermediate (**CI**) in between the first proton transfer of the attacking nucleophile to the assisting amine (**R6**) and the second proton transfer of the assisting amine to the thiocarbonylic sulfur (**R7**). The neutral intermediate (**NI**) can then react to the final products via an unassisted (**R4**), amine-assisted (**R8**), or thiol-assisted (**R11**) reaction. All of the assisted reactions (**R5−11**) have considerably lower enthalpy barriers than the analogous unassisted reactions. Although the loss in entropy is also substantially higher in these reactions, mainly due to the loss of translational entropy of the assisting molecule, this nevertheless leads to Gibbs free energy barriers of the amine-assisted reactions (**R5−9**) that are significantly lower than those of the analogous unassisted reactions (**R2−4**). This lower free energy barrier is due to the formation of a six-membered transition

Table 2. Equilibrium Coefficients (K, Either in L mol^{-1} or Dimensionless), Intrinsic Chemical Forward and Reverse Rate Coefficients (k_+ and k_-, Either in L mol^{-1} s^{-1} or in s^{-1}), Diffusional Contributions (k_{diff} in L mol^{-1} s^{-1}), and Apparent Forward and Reverse Rate Coefficients ($k_{app,+}$ and $k_{app,-}$, Either in L mol^{-1} s^{-1} or in s^{-1}) at 298.15 K in THF for All Elementary Reactions As Shown in Figure 4

reaction	K	k_+	k_-	k_{diff}	$k_{app,+}$	$k_{app,-}$
R1	1.0×10^{-06}	1.3×10^{04}	1.3×10^{10}	2.9×10^{09}	1.3×10^{04}	1.3×10^{10}
R2	3.0×10^{16}	2.3×10^{-04}	7.5×10^{-21}	3.1×10^{09}	2.3×10^{-04}	7.5×10^{-21}
R3	1.6×10^{05}	2.4×10^{00}	1.5×10^{-05}		2.4×10^{00}	1.5×10^{-05}
R4	1.9×10^{11}	4.3×10^{-06}	2.2×10^{-17}	3.1×10^{09}	4.3×10^{-06}	2.2×10^{-17}
R5	3.0×10^{16}	2.2×10^{02}	7.2×10^{-15}	3.2×10^{09}	2.2×10^{02}	7.2×10^{-15}
R6	2.1×10^{00}	6.2×10^{12}	2.9×10^{12}	2.1×10^{09}	2.1×10^{09}	1.0×10^{09}
R7	7.4×10^{04}	5.6×10^{12}	7.6×10^{07}	2.8×10^{09}	5.5×10^{12}	7.4×10^{07}
R8	1.9×10^{11}	3.4×10^{05}	1.8×10^{-06}	3.1×10^{09}	3.4×10^{05}	1.8×10^{-06}
R9	3.0×10^{16}	1.1×10^{-06}	3.6×10^{-23}	3.1×10^{09}	1.1×10^{-06}	3.6×10^{-23}
R10	1.6×10^{05}	7.8×10^{06}	5.0×10^{01}	3.1×10^{09}	7.8×10^{06}	5.0×10^{01}
R11	1.9×10^{11}	4.0×10^{-03}	2.1×10^{-14}	3.1×10^{09}	4.0×10^{-03}	2.1×10^{-14}

DOI: 10.1021/acs.joc.6b01844
J. Org. Chem. 2016, 81, 11626−11634

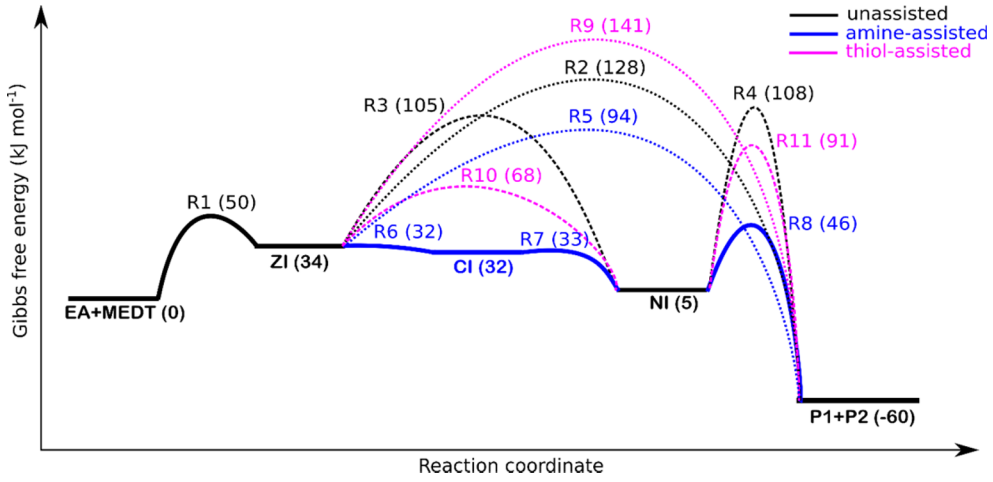

Figure 5. Gibbs free energy diagram at 298.15 K for the various species occurring during the aminolysis of MEDT with EA. Species are labeled according to the reaction scheme shown in Figure 4, and the Gibbs free energies are shown in parentheses (in kJ mol^{-1}) and refer to the reactant level. The bold line shows the minimum Gibbs free energy path.

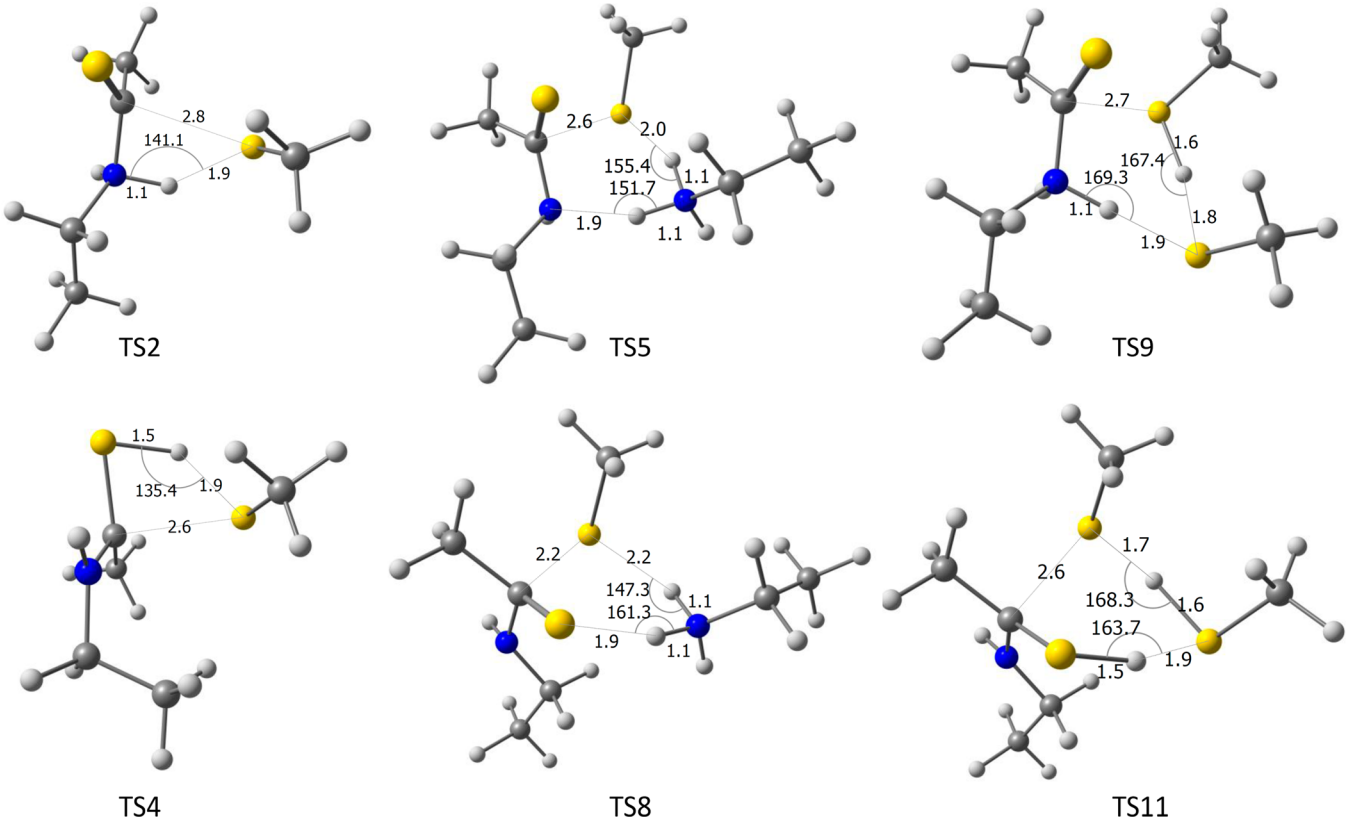

Figure 6. Top: Transition states for the reactions **R2**, **R5**, and **R9**, going from the zwitterionic intermediate (**ZI**) toward the products **P1** and **P2**: unassisted (**TS2**), amine assisted (**TS5**), and thiol assisted (**TS9**). Bottom: Transition states for the reactions **R4**, **R8**, and **R11**, going from the neutral intermediate to the products **P1** and **P2**: unassisted (**TS4**), amine assisted (**TS8**), and thiol assisted (**TS11**).

state that allows proton transfer to occur much more favorably than over the four-membered transition states found in case of unassisted reactions. This is illustrated in Figure 6 for the unassisted (**R4**), amine-assisted (**R8**), and thiol-assisted (**R11**) transition states for the reactions going from the neutral intermediate **NI** to the products **P1** and **P2**.

Using classical transition-state theory, rate coefficients were calculated from the Gibbs free energies reported in Table 1, leading to the intrinsic rate coefficients shown in Table 2. Given that some of the rate coefficients of proton-transfer reactions have a very large value, the rate of these reactions could become diffusion controlled. Hence, a proper evaluation of the observed kinetics requires that diffusional contributions (cf. Table 2) are explicitly taken into account, which is done via the *coupled encounter pair* model (see section S2 in the Supporting Information), in agreement with previous work.[24] This leads to the forward and reverse apparent rate coefficients, $k_{app,+}$ and $k_{app,-}$, respectively, shown in Table 2.

A kinetic model considering all forward and reverse elementary steps is then used to simulate the aminolysis

DOI: 10.1021/acs.joc.6b01844
J. Org. Chem. 2016, 81, 11626−11634

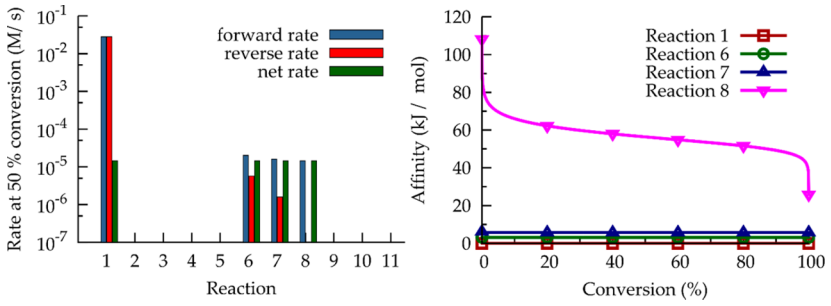

Figure 7. Results of the microkinetic modeling of the aminolysis of MEDT with ethylamine. Left: Forward, reverse, and net rates (logarithmic) of all of the elementary reactions at 50% conversion. Right: Chemical affinity of the elementary reactions involved in the operative reaction mechanism. The reaction are numbered according to Figure 4. Key: $c_{EA,0}$ = 5 mM; $c_{MEDT,0}$ = 1 mM, T = 298.15 K.

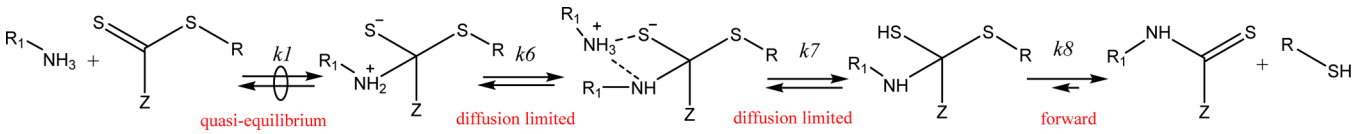

Figure 8. Dominant reaction mechanism for the aminolysis of a RAFT agent.

reaction of MEDT with **EA** in THF at experimentally relevant conditions (cf. Figure S4 in the Supporting Information for concentration profiles). The operative reaction mechanism can readily be determined by analysis of the net rates, r, which are calculated based on the forward, r_+, and reverse rates, r_-, of reaction, according to eqs 1 −3

$$r_+ = k_{app,+} \prod_i [R_i]^{\nu i} \quad (1)$$

$$r_- = k_{app,-} \prod_i [P_i]^{\nu i} \quad (2)$$

$$r = r_+ - r_- \quad (3)$$

where $[R_i]$ and $[P_i]$ refer to the reactants and products of the corresponding elementary reaction with ν_i being their respective stoichiometric coefficient.

Forward, reverse, and net rates at 50% conversion are shown in Figure 7 (left) for relevant reactant concentrations.

Clearly, the mechanism consisting of the elementary steps **R1** and **R6**−**R8** is dominating and is illustrated in Figure 8. The aminolysis of a RAFT agent in an aprotic polar solvent thus occurs via four elementary steps over three intermediate structures: (i) the formation of a zwitterionic intermediate **ZI**, (ii) the formation of a complex intermediate **CI**, in which an assisting amine molecule has taken over the proton from the zwitterionic intermediate, (iii) the breakdown of the complex into a neutral tetrahedral intermediate **NI** with release of the assisting amine molecule, and (iv) the amine-assisted breakdown of the neutral intermediate **NI** into the products **P1** and **P2**.

This is further supported by analyzing the relative contributions of every sequence of elementary steps leading to the formation of the products (cf. Figures S6 and S7 in the Supporting Information for a range of amine and RAFT agent concentrations). Additionally, analysis of the Gibbs free energy diagram (Figure 5) shows that the dominant mechanism coincides with the minimum Gibbs free energy path. Note that this is mostly the case, although not necessarily, since concentration effects are not taken into account in the latter. More information on the nature of the individual elementary steps can be obtained via analysis of the chemical affinities, which can be calculated using the De Donder relation[25] as shown in eq 4:

$$A = RT \ln \frac{r_+}{r_-} \quad (4)$$

The quasi-equilibrated steps are then identified as those having a chemical affinity equal to zero.[25,26] This is the case for reaction **R1**, as shown in Figure 7 (right). Note that reactions **R6** and **R7** are in the diffusion-controlled regime because their apparent rate coefficients are smaller than their intrinsic ones (cf. Table 2). For reaction **R8**, the chemical affinity is significantly larger than zero over the whole course of the reaction, which implies that this reaction is the furthest from equilibrium and can be considered to proceed only in the forward direction in the considered range of conditions.

In a previous experimental study by Deletre et al.,[27] the authors assumed a mechanism composed of three steps: (i) equilibrated formation of a zwitterionic intermediate, (ii) amine-catalyzed proton transfer forming a neutral intermediate, and (iii) rapid breakdown of this neutral intermediate. The theoretical results from this study support this hypothesis very well, with the added nuance that the amine-assisted proton transfer from the zwitterionic intermediate to the neutral intermediate occurs in two diffusion-controlled steps (**R6** and **R7**).

Kinetic Analysis of Commonly Used RAFT Agents. Having determined the operative reaction mechanism for the aminolysis of a model RAFT agent, the thermodynamic and kinetic parameters for this mechanism are calculated for practically used types of RAFT agents, such as dithiobenzoates, trithiocarbonates, xanthates, and dithiocarbamates. For the aminolysis of xanthates or dithiocarbamates (Z = OR′ or NR″R′, respectively), an alternative reaction exists[28] in which the Z group is cleaved off instead of the SR group (or, for macromolecular analogous reactions, the polymeric thiol). This side reaction, leading to a dithiocarbamate and an alcohol (in the case of xanthates) or an amine (in the case of dithiocarbamates), is competing with the desired breakdown of the neutral intermediate (**NI**) into a thiol and a thioamide, as shown in Figure 9. Similar to the breakdown of the neutral

DOI: 10.1021/acs.joc.6b01844
J. Org. Chem. 2016, 81, 11626−11634

intermediate to the desired products (**P1** and **P2**), this side reaction is also assumed to be amine assisted.

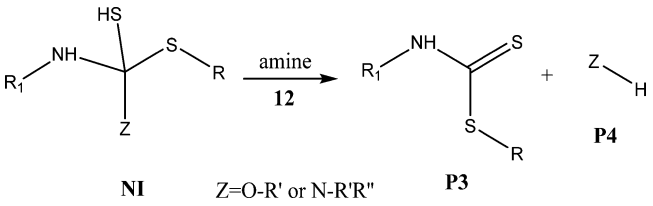

Figure 9. Side reaction occurring during the aminolysis of xanthates (Z = OR′) and dithiocarbamates (Z = NR′R″) in which the Z group of the RAFT agent is cleaved off from the neutral intermediate (**NI**) instead of the thiol, and a dithiocarbamate (**P3**) and an alcohol or amine (**P4**) are formed.

In the case of trithiocarbonates (Z = SR′), there is the possibility that not the polymeric thiol is cleaved off but the thiol corresponding to the Z group. In that case, the macro-RAFT agent will convert to a macro-dithiocarbamate (see section S8 in the Supporting Information). Reaction and activation enthalpies, entropies, Gibbs free energies, and forward and reverse rate coefficients at 298.15 K in THF are calculated along the dominant path for a dithiobenzoate (EDTB), a trithiocarbonate (DETTC), a xanthate (DEX), and a dithiocarbamate (EDMDTC) and are shown in Table 3. For the latter two RAFT agents (DEX and EDMDTC), these data are also presented for the side reaction (**R12**).

As expected, the Z group plays a significant influence on the energy barrier of the formation of the zwitterionic intermediate. This is reflected in the energy of the lowest unoccupied molecular orbitals (LUMO) in the gas phase of the various RAFT agents, as shown in Figure 10. When this value is compared with the activation enthalpy in the gas phase (cf. Table S5 in the Supporting Information), a qualitative correlation can be obtained as is shown in Figure 11 (left).

Additionally, there is also a relation between the activation enthalpy and the reaction enthalpy in the gas phase (Figure 11 (right)). Hence, the LUMO is also qualitatively correlated with the reaction enthalpy of the first elementary reaction.

The other steps, involving proton transfer, are less influenced by the nature of the Z group since it is known that proton-transfer reactions are heavily influenced by the angle over which they take place,[29] and this is largely unaffected by the type of Z group.

Apparent rate coefficients based on the ab initio parameters (Table 3) and including the relevant diffusional contributions (Table 2) are shown in Table 4.

These kinetic parameters are again used in a microkinetic model, now to simulate the reaction at experimental conditions used in literature in good agreement with the reported findings (cf. Table S10 in the Supporting Information for details).[3,4,30,31] In particular, comparison with kinetic experiments on xanthates and dithiobenzoates by Kabachii and Kochev[30] show that simulated conversions deviate less than a factor of 2. Taking into account that the reaction parameters are solely obtained using theoretical methods, this is a very satisfactory result and exemplifies the predictive power of theoretical modeling. It should be mentioned that the other comparisons involve experimental studies[3,4,31] that where aimed at obtaining complete conversions, and, unfortunately, these experimental studies provided no details on the kinetics of the reaction. The simulated results indicated that in these cases complete conversion was obtained well within the reported times.

Furthermore, for xanthates the formation of side product has been simulated and is shown to be considerably slower than the formation of the main product. The forward apparent rate coefficient at room temperature, $k_{app,+}$, for DEX-R12 is 4.0×10^{02} L mol^{-1} s^{-1}, while for DEX-R8 this is 3.2×10^{05} L mol^{-1} s^{-1} (Table 4). The yield of side product is hence ignorable, and the simulations show a ratio of 1.25×10^{-3}:1 to the main products at 100% conversion (see Figure S19 in the Supporting

Table 3. Standard Reaction Enthalpy, Entropy, and Gibbs Free Energy ($\Delta_rH°$, $\Delta_rS°$, $\Delta_rG°$ in, Respectively, kJ mol^{-1}, J mol^{-1} K^{-1}, kJ mol^{-1}), Standard Activation Enthalpy, Entropy and Gibbs Free Energy ($\Delta^{‡}H°$, $\Delta^{‡}S°$, $\Delta^{‡}G°$ in, Respectively, kJ mol^{-1}, J mol^{-1} K^{-1}, kJ mol^{-1}), and Intrinsic Chemical Forward and Reverse Rate Coefficients ($k_{app,+}$ and $k_{app,-}$ in mol L^{-1} s^{-1} or s^{-1}) at 298.15 K in THF (Reference State is 1 mol L^{-1}) for the Elementary Reactions along the Dominant Path (R1, R6−R8) for the Aminolysis of DTB, DETTC, DEX, and EDMDTC with EA as Well as for the Side Reaction (R12) for DEX and EDMDTC

reaction	$\Delta_rH°$	$\Delta_rS°$	$\Delta_rG°$	$\Delta^{‡}H°$	$\Delta^{‡}S°$	$\Delta^{‡}G°$
EDTB-R1	−11.7	−162.9	36.9	1.1	−162.2	49.5
EDTB-R6	−35.3	−102.6	−4.7	−33.1	−104.7	−1.9
EDTB-R7	22.5	145.8	−21.0	4.2	10.7	1.0
EDTB-R8	−42.7	97.4	−71.8	−5.6	−141.4	36.5
DETTC-R1	−1.8	−163.0	46.8	23.6	−154.6	69.7
DETTC-R6	−40.2	−98.8	−10.7	−37.8	−97.8	−8.7
DETTC-R7	32.7	144.6	−10.4	9.5	13.2	5.5
DETTC-R8	−52.3	99.5	−81.9	−16.3	−166.0	33.2
DEX-R1	−6.6	−163.5	42.1	30.3	−140.5	72.2
DEX-R6	−23.6	−95.2	4.8	−24.8	−93.3	3.0
DEX-R7	23.4	150.8	−21.6	9.1	15.0	4.6
DEX-R8	−59.8	104.7	−91.0	−1.4	−144.2	41.6
DEX-R12	−64.3	61.5	−82.6	13.1	−151.2	58.2
EDMDTC-R1	39.1	−165.6	88.5	49.6	−164.4	98.7
EDMDTC-R6	−28.4	−100.7	1.6	−26.3	−98.0	2.9
EDMDTC-R7	9.6	140.0	−32.1	6.7	14.7	2.4
EDMDTC-R8	−61.1	122.7	−97.7	−8.0	−139.6	33.7
EDMDTC-R12	−29.7	120.0	−65.4	−14.3	−155.9	32.1

DOI: 10.1021/acs.joc.6b01844
J. Org. Chem. 2016, 81, 11626−11634

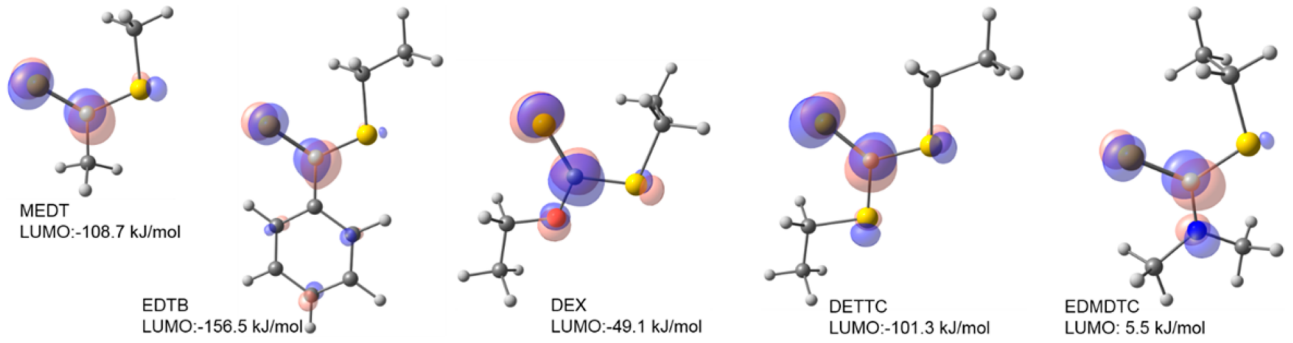

Figure 10. Lowest unoccupied molecular orbitals (LUMO) for MEDT, EDTB, DETTC, DEX, and EDMDTC calculated at the M06-2X/6-311+G(d,p) level of theory in the gas phase.

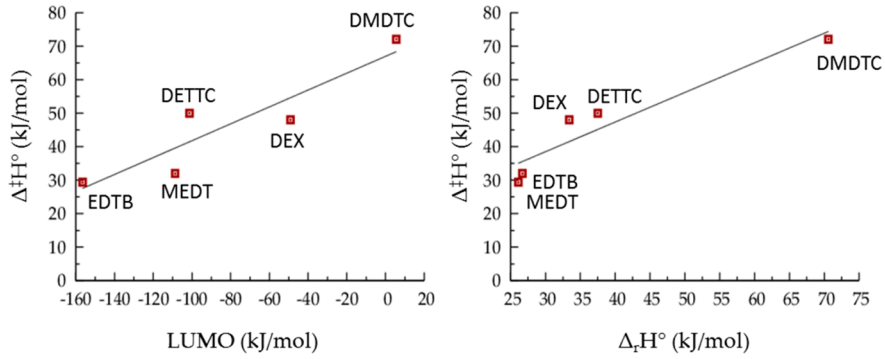

Figure 11. Left: Standard activation enthalpy ($\Delta^{\ddagger}H°$) of the formation of the zwitterionic intermediate (**TS1**) versus the energy of the LUMO of the RAFT agent in the gas phase (R^2 = 0.84). Right: Standard activation enthalpy ($\Delta^{\ddagger}H°$) of the formation of the zwitterionic intermediate (**TS1**) versus the standard reaction enthalpy for the aminolysis reactions of the different RAFT agents in the gas phase (R^2 = 0.90).

Table 4. Equilibrium Coefficients (K, Either in L mol^{-1} or Dimensionless), Intrinsic Chemical Forward and Reverse Rate Coefficients (k_+ and k_-, Either in L mol^{-1} s^{-1} or in s^{-1}), Diffusional Contributions (k_{diff} in L mol^{-1} s^{-1}), and Apparent Forward and Reverse Rate Coefficients ($k_{app,+}$ and $k_{app,-}$ Either in L mol^{-1} s^{-1} or in s^{-1}) at 298.15 K in THF for the Elementary Reactions along the Dominant Path (R1 and R6−R8) for the Aminolysis of EDTB, DETTC, DEX, and EDMDTC as Well as for the Side Reaction (R12) for DEX and EDMDTC

reaction	K	k_+	k_-	k_{diff}	$k_{app,+}$	$k_{app,-}$
EDTB-R1	3.5×10^{-07}	1.3×10^{04}	3.8×10^{10}	3.1×10^{09}	1.3×10^{04}	3.8×10^{10}
EDTB-R6	6.7×10^{00}	6.2×10^{12}	9.3×10^{11}	1.5×10^{09}	1.5×10^{09}	2.2×10^{08}
EDTB-R7	4.8×10^{03}	4.2×10^{12}	8.7×10^{08}	1.4×10^{09}	2.5×10^{12}	5.3×10^{08}
EDTB-R8	3.8×10^{12}	2.5×10^{06}	6.5×10^{-07}	6.4×10^{08}	2.5×10^{06}	6.5×10^{-07}
DETTC-R1	6.2×10^{-09}	3.9×10^{00}	6.2×10^{08}	3.1×10^{09}	3.9×10^{00}	6.2×10^{08}
DETTC-R6	7.6×10^{01}	6.2×10^{12}	8.2×10^{10}	1.5×10^{09}	1.5×10^{09}	1.9×10^{07}
DETTC-R7	6.7×10^{01}	6.7×10^{11}	1.0×10^{10}	1.4×10^{09}	8.0×10^{10}	1.2×10^{09}
DETTC-R8	2.3×10^{14}	9.6×10^{06}	4.3×10^{-08}	6.4×10^{08}	9.5×10^{06}	4.2×10^{-08}
DEX-R1	4.2×10^{-08}	1.4×10^{00}	3.4×10^{07}	3.1×10^{09}	1.4×10^{00}	3.4×10^{07}
DEX-R6	1.5×10^{-01}	1.8×10^{12}	1.3×10^{13}	1.5×10^{09}	1.5×10^{09}	1.0×10^{10}
DEX-R7	6.0×10^{03}	9.7×10^{11}	1.6×10^{08}	1.4×10^{09}	8.7×10^{11}	1.5×10^{08}
DEX-R8	8.9×10^{15}	3.2×10^{05}	3.5×10^{-11}	6.4×10^{08}	3.2×10^{05}	3.5×10^{-11}
DEX-R12	3.0×10^{14}	4.0×10^{02}	1.3×10^{-12}	6.4×10^{08}	4.0×10^{02}	1.3×10^{-12}
EDMDTC-R1	3.1×10^{-16}	3.2×10^{-05}	1.0×10^{11}	3.1×10^{09}	3.2×10^{-05}	1.0×10^{11}
EDMDTC-R6	5.3×10^{-01}	1.9×10^{12}	3.6×10^{12}	1.5×10^{09}	1.5×10^{09}	2.8×10^{09}
EDMDTC-R7	4.3×10^{05}	2.4×10^{12}	5.6×10^{06}	1.4×10^{09}	2.4×10^{12}	5.6×10^{06}
EDMDTC-R8	1.3×10^{17}	7.9×10^{06}	5.9×10^{-11}	6.4×10^{08}	7.8×10^{06}	5.8×10^{-11}
EDMDTC-R12	2.9×10^{11}	1.5×10^{07}	5.0×10^{-05}	6.4×10^{08}	1.4×10^{07}	4.9×10^{-05}

Information for concentration profiles). This can be rationalized by the fact that thiolates are better leaving groups than alkoxides.

No conversion was found to take place for the aminolysis of dithiocarbamates in a range of conditions. (cf. Figure S23 in the Supporting Information for $c_{EA,0}$ = 5 mM; $c_{EDMDTC,0}$ = 1 mM, T = 298.15 K) as could have been predicted on the basis of the correlations shown in Figure 11. This is validated by the previous experimental results of Le Neindre et al.,[32] who found that at room temperature dithiocarbamates indeed do not undergo aminolysis at experimentally practical conditions. In that study, it was thus concluded that dithiocarbamates were

DOI: 10.1021/acs.joc.6b01844
J. Org. Chem. 2016, 81, 11626−11634

unfit to serve as thiol-protecting groups. As far as the reaction path analysis goes, similar conclusions can be drawn as for MEDT, except for DEX, where **R6** is no longer rate controlling. Lastly, the conversion profiles of each of the RAFT agents have been simulated at the same set of conditions, i.e., starting concentrations of 1 mM RAFT agent and 5 mM amine (cf. Figure S12 in the Supporting Information). The order of reactivity is shown to be dithioate ≥ dithiobenzoate > xanthate ≥ trithiocarbonate ≫ dithiocarbamate, correlating with the equilibrium coefficient of the first elementary reaction, the formation of the zwitterionic intermediate.

3. CONCLUSION

A detailed complete reaction network for the aminolysis of a model RAFT agent (Z = CH_3) has been presented together with kinetic and thermodynamic data for every step. An ab initio based kinetic model has been constructed, revealing a dominant path involving several intermediate structures: a zwitterionic intermediate, a complex intermediate with another amine which facilitates the proton transfer, and a neutral tetrahedral intermediate. Except for the formation of the zwitterionic intermediate, all of the other steps that involve proton transfer are amine assisted, confirming previous conclusions on the aminolysis reactions in aprotic solvents of other molecules, such as thiolactones[17] or anhydrides.[20] In this reaction mechanism, the formation of the complex intermediate is diffusion controlled. Furthermore, a kinetic analysis for the aminolysis reaction of four other, commonly used, RAFT agents was performed. Alkanedithioates were found to react the fastest, closely followed by dithiobenzoates, trithiocarbonates, and xanthates that react considerably slower, and for dithiocarbamates, no reaction takes place at experimentally relevant concentrations (1−100 mM). This order of reactivity approximately correlates with the reaction Gibbs free energy of the zwitterionic intermediate formed during the first elementary step. Furthermore, for xanthates, the side reaction in which the Z group is cleaved off was found to be considerably slower than the main reaction. This corresponds with the fact that alkoxide groups are known to be poor leaving groups. Overall, the presented study not only offers qualitative insight in the reaction mechanism of a widely used synthetic procedure but also delivers quantitative thermodynamic and kinetic parameters of all of the elementary steps for various RAFT agents.

4. COMPUTATIONAL METHODS

All the electronic structure calculations are performed using the Gaussian-09 package.[33] Global minimum energy conformations for reactants, products, and intermediates are determined by rotating all dihedral angles at the B3LYP/6-31G(d) level of theory. All thermal contributions were calculated in the harmonic oscillator approach. Electronic energies were calculated using a single-point calculation at the M06-2X/6-311+G(d,p) level of theory on the B3LYP/6-31G(d)-optimized geometries. M06-2X is a hybrid meta density functional designed for main-group thermochemistry and kinetics[34] and has been used for the calculation of aminolysis[35,36] and similar[37,38] reactions before. For the optimization of transition states, the Berny algorithm is applied.[39] Minimum energy conformations and transition states are confirmed to have zero and one imaginary frequency, respectively. Gibbs free energies of solvation in THF, $\Delta_{solv}G°$, were calculated using COSMO-RS[40] theory as implemented in the COSMOtherm[41] software, version C30_1301, based on BP86/TZVP calculations on the B3LYP/6-31G(d)-optimized structures, as this is the level of theory to which COSMO-RS is parametrized.

A detailed procedure explaining the ab initio calculation of enthalpies, entropies, Gibbs free energies, equilibrium coefficients, and intrinsic chemical rate coefficients in this work can be found in section S1 of the Supporting Information. Furthermore, in order to obtain apparent rate coefficients, diffusional contributions were taken into account according to the encounter pair model,[24,42] which is further elaborated in section S2 of the Supporting Information.

The microkinetic model was constructed on the basis of the reaction scheme shown in Figure 4 including the side reaction shown in Figure 9 for DEX and EDMTC (see section S10 in the Supporting Information for the corresponding continuity equations). Integration was performed using the LSODA algorithm (i.e., Livermore Solver for Ordinary Equations).[43]

■ ASSOCIATED CONTENT

Supporting Information

The Supporting Information is available free of charge on the ACS Publications website at DOI: 10.1021/acs.joc.6b01844.

Details on the computational procedures, details on the coupled encounter pair model, diffusion coefficients and diffusional contributions, thermodynamic and kinetic data in gas phase, simulated concentration profiles, fractional contributions to the conversion, net rates and affinities, details on possible side reactions, a comparison between simulated results and results reported in literature, continuity equations, and Cartesian coordinates of all stationary points (PDF)

■ AUTHOR INFORMATION

Corresponding Author

*E-mail: mariefrancoise.reyniers@ugent.be.

Notes

The authors declare no competing financial interest.

■ ACKNOWLEDGMENTS

We acknowledge financial support from Long-term Structural Methusalem Funding by the Flemish Government, the Interuniversity Attraction Poles Programme - Belgian State - Belgian Science Policy, and the Fund for Scientific Research Flanders (FWO; G.045212N; G.0065.13N). D.R.D. acknowledges the Fund for Scientific Research Flanders (FWO) through a postdoctoral fellowship. The computational work was carried out using the STEVIN Supercomputer Infrastructure at Ghent University, funded by Ghent University, the Flemish Supercomputer Center (VSC), the Hercules Foundation, and the Flemish Government, Department EWI.

■ REFERENCES

(1) Chiefari, J.; Chong, Y. K.; Ercole, F.; Krstina, J.; Jeffery, J.; Le, T. P. T.; Mayadunne, R. T. A.; Meijs, G. F.; Moad, C. L.; Moad, G.; Rizzardo, E.; Thang, S. H. *Macromolecules* **1998**, *31*, 5559.
(2) Willcock, H.; O'Reilly, R. K. *Polym. Chem.* **2010**, *1*, 149.
(3) Vandenbergh, J.; Tura, T.; Baeten, E.; Junkers, T. *J. Polym. Sci., Part A: Polym. Chem.* **2014**, *52*, 1263.
(4) Qiu, X.-P.; Winnik, F. M. *Macromol. Rapid Commun.* **2006**, *27*, 1648.
(5) Moad, G.; Chong, Y. K.; Postma, A.; Rizzardo, E.; Thang, S. H. *Polymer* **2005**, *46*, 8458.
(6) Nicolaÿ, R. *Macromolecules* **2012**, *45*, 821.
(7) Derboven, P.; D'hooge, D. R.; Stamenovic, M. M.; Espeel, P.; Marin, G. B.; Du Prez, F. E.; Reyniers, M.-F. *Macromolecules* **2013**, *46*, 1732.
(8) Hoyle, C. E.; Bowman, C. N. *Angew. Chem., Int. Ed.* **2010**, *49*, 1540.

DOI: 10.1021/acs.joc.6b01844
J. Org. Chem. 2016, 81, 11626−11634

(9) Nair, D. P.; Podgorski, M.; Chatani, S.; Gong, T.; Xi, W. X.; Fenoli, C. R.; Bowman, C. N. *Chem. Mater.* **2014**, *26*, 724.
(10) Chan, J. W.; Hoyle, C. E.; Lowe, A. B.; Bowman, M. *Macromolecules* **2010**, *43*, 6381.
(11) Lammens, M.; Du Prez, F. In *Complex Macromolecular Architectures*; John Wiley & Sons, 2011; p 229.
(12) Xiong, X. Q.; Tang, Z. K.; Cai, L. *Prog. Chem.* **2012**, *24*, 1751.
(13) Binder, W. H.; Sachsenhofer, R. *Macromol. Rapid Commun.* **2007**, *28*, 15.
(14) Coote, M. L. *J. Phys. Chem. A* **2005**, *109*, 1230.
(15) Izgorodina, E. I.; Coote, M. L. *J. Phys. Chem. A* **2006**, *110*, 2486.
(16) Lin, C. Y.; Marque, S. R. A.; Matyjaszewski, K.; Coote, M. L. *Macromolecules* **2011**, *44*, 7568.
(17) Desmet, G. B.; D'hooge, D. R.; Sabbe, M. K.; Marin, G. B.; Du Prez, F. E.; Espeel, P.; Reyniers, M.-F. *J. Org. Chem.* **2015**, *80*, 8520.
(18) Hogan, J. C.; Gandour, R. D. *J. Org. Chem.* **1991**, *56*, 2821.
(19) Rao, H.-B.; Wang, Y.-Y.; Zeng, X.-Y.; Xue, Y.; Li, Z.-R. *Comput. Theor. Chem.* **2013**, *1008*, 8.
(20) Petrova, T.; Okovytyy, S.; Gorb, L.; Leszczynski, J. *J. Phys. Chem. A* **2008**, *112*, 5224.
(21) Truhlar, D. G.; Garrett, B. C. *Acc. Chem. Res.* **1980**, *13*, 440.
(22) Sung, D. D.; Koo, I. S.; Yang, K.; Lee, I. *Chem. Phys. Lett.* **2006**, *426*, 280.
(23) Sung, D. D.; Koo, I. S.; Yang, K.; Lee, I. *Chem. Phys. Lett.* **2006**, *432*, 426.
(24) D'Hooge, D. R.; Reyniers, M.-F.; Marin, G. B. *Macromol. React. Eng.* **2013**, *7*, 362.
(25) De Donder, T.; Van Rysselberghe, P.*Thermodynamic theory of affinity*; Stanford University Press, 1936; Vol. *1*.
(26) Marin, G.; Yablonsky, G. S.*Kinetics of chemical reactions*; John Wiley & Sons, 2011.
(27) Deletre, M.; Levesque, G. *Macromolecules* **1990**, *23*, 4733.
(28) Barrett, G. C.; Martins, C. M. O. A. *J. Chem. Soc., Chem. Commun.* **1972**, 638.
(29) Wang, L.-H.; Zipse, H. *Liebigs Ann.* **1996**, *1996*, 1501.
(30) Kabachii, Y. A.; Kochev, S. Y. *Polym. Sci., Ser. A* **2006**, *48*, 717.
(31) Boyer, C.; Granville, A.; Davis, T. P.; Bulmus, V. *J. Polym. Sci., Part A: Polym. Chem.* **2009**, *47*, 3773.
(32) Le Neindre, M.; Magny, B.; Nicolay, R. *Polym. Chem.* **2013**, *4*, 5577.
(33) Frisch, M. J.; Trucks, G. W.; Schlegel, H. B.; Scuseria, G. E.; Robb, M. A.; Cheeseman, J. R.; Scalmani, G.; Barone, V.; Mennucci, B.; Petersson, G. A.; Nakatsuji, H.; Caricato, M.; Li, X.; Hratchian, H. P.; Izmaylov, A. F.; Bloino, J.; Zheng, G.; Sonnenberg, J. L.; Hada, M.; Ehara, M.; Toyota, K.; Fukuda, R.; Hasegawa, J.; Ishida, M.; Nakajima, T.; Honda, Y.; Kitao, O.; Nakai, H.; Vreven, T.; Montgomery, J. A., Jr.; Peralta, J. E.; Ogliaro, F.; Bearpark, M.; Heyd, J. J.; Brothers, E.; Kudin, K. N.; Staroverov, V. N.; Kobayashi, R.; Normand, J.; Raghavachari, K.; Rendell, A.; Burant, J. C.; Iyengar, S. S.; Tomasi, J.; Cossi, M.; Rega, N.; Millam, J. M.; Klene, M.; Knox, J. E.; Cross, J. B.; Bakken, V.; Adamo, C.; Jaramillo, J.; Gomperts, R.; Stratmann, R. E.; Yazyev, O.; Austin, A. J.; Cammi, R.; Pomelli, C.; Ochterski, J. W.; Martin, R. L.; Morokuma, K.; Zakrzewski, V. G.; Voth, G. A.; Salvador, P.; Dannenberg, J. J.; Dapprich, S.; Daniels, A. D.; Farkas; Foresman, J. B.; Ortiz, J. V.; Cioslowski, J.; Fox, D. J. *Gaussian 09*; Gaussian, Inc.: Wallingford CT, 2009.
(34) Zhao, Y.; Truhlar, D. G. *Theor. Chem. Acc.* **2008**, *120*, 215.
(35) Mandal, D.; Sen, K.; Das, A. K. *J. Phys. Chem. A* **2012**, *116*, 8382.
(36) Ilieva, S.; Nalbantova, D.; Hadjieva, B.; Galabov, B. *J. Org. Chem.* **2013**, *78*, 6440.
(37) Lawal, M. M.; Govender, T.; Maguire, G. E. M.; Honarparvar, B.; Kruger, H. G. *J. Mol. Model.* **2016**, *22*, 1.
(38) Swiderek, K.; Tunon, I.; Marti, S.; Moliner, V.; Bertran, J. *J. Am. Chem. Soc.* **2013**, *135*, 8708.
(39) Schlegel, H. B. *J. Comput. Chem.* **1982**, *3*, 214.
(40) Klamt, A.; Eckert, F. *Fluid Phase Equilib.* **2000**, *172*, 43.
(41) Diedenhofen, M.; Hellweg, A.; Huniar, U.; Klamt, A.; Loschen, C.; Reinisch, J.; Schroer, A.; Steffen, C.; Thomas, K.; Wichmann, K.; Ikeda, H. *COSMOtherm*, version version C30_1601; COSMOlogic: Leverkusen, 2013.
(42) de Kock, J. B. L.; Van Herk, A. M.; German, A. L. *J. Macromol. Sci., Polym. Rev.* **2001**, *41*, 199.
(43) Petzold, L. *Siam J. Sci. Stat Comput* **1983**, *4*, 136.

DOI: 10.1021/acs.joc.6b01844
J. Org. Chem. 2016, 81, 11626−11634